

Escher-like quasiperiodic heterostructures

This article has been downloaded from IOPscience. Please scroll down to see the full text article.

2009 J. Phys. A: Math. Theor. 42 192002

(<http://iopscience.iop.org/1751-8121/42/19/192002>)

View [the table of contents for this issue](#), or go to the [journal homepage](#) for more

Download details:

IP Address: 171.66.16.153

The article was downloaded on 03/06/2010 at 07:38

Please note that [terms and conditions apply](#).

FAST TRACK COMMUNICATION

Escher-like quasiperiodic heterostructures

A G Barriuso¹, J J Monzón¹, L L Sánchez-Soto¹ and A F Costa²¹ Departamento de Óptica, Facultad de Física, Universidad Complutense, 28040 Madrid, Spain² Departamento de Matemáticas Fundamentales, Facultad de Ciencias, Universidad Nacional de Educación a Distancia, Senda del Rey 9, 28040 Madrid, Spain

Received 2 February 2009, in final form 25 March 2009

Published 22 April 2009

Online at stacks.iop.org/JPhysA/42/192002**Abstract**

Quasiperiodic heterostructures present unique structural, electronic and vibrational properties, connected to the existence of incommensurate periods. We go beyond previous schemes, such as Fibonacci or Thue–Morse, based on substitutional sequences, by introducing construction rules generated by tessellations of the unit disc by regular polygons. We explore some of the properties exhibited by these systems.

PACS numbers: 61.44.Br, 68.65.Cd, 71.55.Jv, 78.67.Pt

(Some figures in this article are in colour only in the electronic version)

Quasiperiodic (QP) systems have been receiving a lot of attention over the last few years (Maciá 2006). The interest was originally fueled by the theoretical predictions that they should manifest peculiar electron and phonon critical states (Ostlund and Pandit 1984, Kohmoto *et al* 1987), associated with highly fragmented fractal energy spectra (Kohmoto *et al* 1983, Sütö 1989, Bellissard *et al* 1989, Chakrabarti *et al* 1995, Liu 1997). On the other hand, practical fabrication of Fibonacci (Merlin *et al* 1985) and Thue–Morse (Merlin *et al* 1987) superlattices triggered a number of experimental achievements that have provided new insights into the capabilities of QP structures (Velasco and García-Moliner 2003). In particular, possible optical applications have deserved major attention and some intriguing properties have been demonstrated (Tamura and Nori 1989, Hattori *et al* 1994, Vasconcelos and Albuquerque 1999, Lusk *et al* 2001, Barriuso *et al* 2005). Underlying all these theoretical and experimental efforts, a crucial fundamental question remains concerning whether QP devices would achieve better performance than the usual periodic ones for some specific applications (Maciá 2001).

The QP arrangements considered thus far rely on substitutional rules among the elements of a basic alphabet. In the common case of a two-letter alphabet $\{A, B\}$, the algorithm takes the form $A \mapsto \sigma_A(A, B)$, $B \mapsto \sigma_B(A, B)$, where σ_A and σ_B can be any string of the letters. The sequences generated after n applications of the algorithm are of significance in fields as diverse as cryptography, time-series analysis and cellular automata (Cheng and Savit 1990). They present unique characteristics, connected to the existence of incommensurate periods. In fact, these systems with two (or more) competing periodicities may exhibit metallic (with Bloch-type extended wavefunctions), insulating (with exponentially localized wavefunctions)

as well as critical phases. In addition, they have interesting algebraic properties, which are usually characterized by the nature of their Fourier or multifractal spectra (Spinadel 1999).

We wish to deal with QP systems from a radically novel perspective. Our starting point is the observation that in many problems of physical interest (Maciá and Rodríguez-Oliveros 2006), the letters of the alphabet can be identified with one-dimensional linear lossless systems (i.e. with two input and two output channels). Under these general conditions, it turns out that the associated transfer matrix belongs to the group $SU(1,1)$, which is also the basic symmetry group of the hyperbolic geometry (Coxeter 1968). In consequence, the unit disc appears as the natural arena to discuss their performance (Yonte *et al* 2002, Monzón *et al* 2002, Barriuso *et al* 2003). Since in the Euclidean plane, QP behavior is intimately linked with tessellations, one is unfailingly led to consider the role of hyperbolic tessellations in the unit disc, much in the spirit of Escher's masterpiece woodcut *Circle Limit III*³ (Coxeter 1996). The answer we propose seems quite promising: the tessellations by different regular polygons provide new sequences with entrancing properties that may open avenues of research in this field.

A QP system can thus be seen as a word obtained by stacking different letters of the basic alphabet. Although our theory applies to a variety of models described by a transfer matrix (Griffiths and Steinke 2001, Pérez-Álvarez *et al* 2001), we deal with a specific realization and focus our attention on the optical response of a lossless superlattice. Let us consider one of these letters (which in practice can be made of several plane-parallel layers), which we assume to be sandwiched between two semi-infinite identical ambient (a) and substrate (s). We suppose monochromatic plane waves incident from both the ambient and the substrate. As a result of multiple reflections in all the interfaces, the total electric field can be decomposed in terms of forward- and backward-traveling plane waves, denoted by $E^{(+)}$ and $E^{(-)}$, respectively (Yeh 1988). If we take these components as a vector $\mathbf{E} = (E^{(+)}, E^{(-)})^t$, then the amplitudes at both the ambient and the substrate sides are related by the transfer matrix \mathbf{M} :

$$\mathbf{E}_a = \mathbf{M}\mathbf{E}_s. \quad (1)$$

It can be shown that \mathbf{M} is of the form (Monzón *et al* 2002)

$$\mathbf{M} = \begin{pmatrix} 1/T & R^*/T^* \\ R/T & 1/T^* \end{pmatrix}, \quad (2)$$

where the complex numbers R and T are, respectively, the overall reflection and transmission coefficients for a wave incident from the ambient. The condition $\det \mathbf{M} = +1$ is equivalent to the energy conservation $|R|^2 + |T|^2 = 1$, and then the set of transfer matrices reduces to the group $SU(1,1)$. Obviously, the matrix of a word obtained by putting letters together is the product of the matrices representing each one of them, taken in an appropriate order.

To proceed further, we note that in many instances we are interested in the transformation properties of field quotients rather than the fields themselves. Therefore, it seems natural to consider the complex numbers

$$z = \frac{E^{(-)}}{E^{(+)}} \quad (3)$$

for both ambient and substrate. The action of the matrix given in equation (1) can then be seen as a function $z_a = f(z_s)$ that can be appropriately called the transfer function. From a geometrical viewpoint, this function defines a transformation of the complex plane \mathbb{C} , mapping the point z_s into the point z_a according to

$$z_a = \frac{\beta^* + \alpha^* z_s}{\alpha + \beta z_s}, \quad (4)$$

³ For more details, the reader can visit the web site www.mcescher.com.

where $\alpha = 1/T$ and $\beta = R^*/T^*$. When no light is incident from the substrate, $z_s = 0$ and then $z_a = R$. Equation (4) is a Möbius transformation: a map of this form is an orientation-preserving isometry that leaves invariant the unit disc with the hyperbolic metric. In this way, we are naturally led to the Poincaré disc model of hyperbolic geometry in which a line is represented as an arc of a circle whose endpoints are orthogonal to the boundary of the disc (Coxeter 1968). We have three different kinds of pairs of lines: intersecting, parallel (they intersect at infinity, which is precisely the boundary of the disc) and ultraparallel (they are neither intersecting nor parallel).

The idea of fixed points proves to be essential. These points are defined as the field configurations such that $z_a = z_s \equiv z$ in equation (4), whose solutions are

$$z = \frac{1}{2\beta} \left\{ -2i \operatorname{Im}(\alpha) \pm \sqrt{[\operatorname{Tr}(\mathbf{M})]^2 - 4} \right\}. \tag{5}$$

The trace then provides a suitable tool for the classification of the system action.

When $[\operatorname{Tr}(\mathbf{M})]^2 < 4$, the action is elliptic and it has only one fixed point inside the unit disc. Since in the Euclidean geometry a rotation is characterized by having only one invariant point, this action can be appropriately called a hyperbolic rotation.

When $[\operatorname{Tr}(\mathbf{M})]^2 > 4$, the action is hyperbolic and it has two fixed points, both on the boundary of the unit disc. The geodesic line joining these two fixed points remains invariant and thus, by analogy with the Euclidean case, this action is called a hyperbolic translation.

Finally, when $[\operatorname{Tr}(\mathbf{M})]^2 = 4$ the action is parabolic and it has only one (double) fixed point on the boundary of the unit disc.

The notion of periodicity is intimately connected with tessellations, i.e. tilings by identical replicas of a unit cell (or fundamental domain) that fill the plane with no overlaps and no gaps. Of special interest is the case when the primitive cell is a regular polygon with a finite area (Zieschang *et al* 1980). In the Euclidean plane, the associated regular tessellation is generically noted $\{p, q\}$, where p is the number of polygon edges and q is the number of polygons that meet at a vertex. We recall that geometrical constraints limit the possible regular tilings $\{p, q\}$ to those verifying $(p - 2)(q - 2) = 4$. This includes the classical tilings $\{4, 4\}$ (tiling by squares) and $\{6, 3\}$ (tiling by hexagons), plus a third one, the tiling $\{3, 6\}$ by triangles (which is dual to $\{6, 3\}$).

In contrast, in the hyperbolic disc regular tilings exist provided $(p - 2)(q - 2) > 4$, which now leads to an infinite number of possibilities (Magnus 1974). The fundamental polygons are connected to the discrete subgroups of isometries (or congruent mappings): they are called Fuchsian groups (Ford 1972) and play for the hyperbolic geometry a role similar to that of crystallographic groups for the Euclidean geometry (Beardon 1983).

A tessellation of the hyperbolic plane by regular polygons has a symmetry group that is generated by reflections in geodesics, which are inversions across circles in the unit disc. These geodesics correspond to edges or axes of symmetry of the polygons. Therefore, to construct a tessellation of the unit disc one just has to build one tile and duplicate it by using reflections in the edges.

To illustrate these ideas, we consider a simple yet nontrivial example of a tessellation by squares with vertices in the unit circle, although the treatment can be immediately extended to other polygons. To this end, we construct the Fuchsian group generated by two parabolic transformations whose fixed points are at two opposite vertices of the fundamental hyperbolic square (centered at the origin). In this way, we get

$$\mathbf{A} = \begin{pmatrix} 1 - i & 1 \\ 1 & 1 + i \end{pmatrix}, \quad \mathbf{B} = \begin{pmatrix} 1 + i & 1 \\ 1 & 1 - i \end{pmatrix}. \tag{6}$$

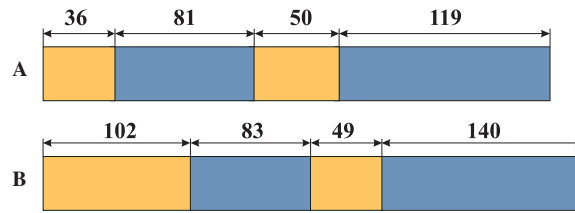


Figure 1. A realistic implementation of the generators **A** and **B** of the tessellation by hyperbolic squares generated by (6). The blue layers are made of cryolite (Na_3AlF_6), while the brown ones are zinc selenide (ZnSe). The wavelength in vacuum is $\lambda = 610$ nm and normal incidence (from left to right) has been assumed. The corresponding thicknesses are expressed in nanometers.

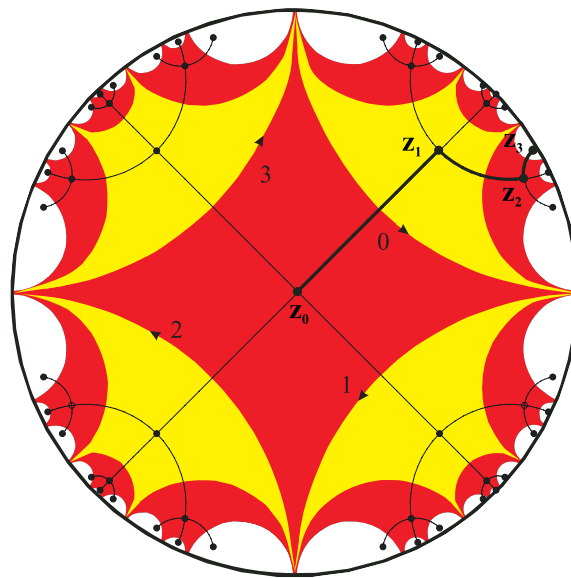


Figure 2. Tessellation of the unit disc with the matrices (6). The marked points are the centers of the squares. All of them are a transformation of the origin by a matrix that have as a reflection coefficient the complex number that links the origin with the center of the square.

The fixed point of **A** is $+i$ and that of **B** is $-i$. In figure 1, we show a possible way in which these matrices can be implemented in terms of two commonly employed materials in optics. Note that, in physical terms, the inverses must be constructed as independent systems.

In figure 2, we have plotted the tessellation obtained by transforming the fundamental square with the Fuchsian group generated by the powers of $\{\mathbf{A}, \mathbf{B}\}$ (and the inverses). The vertices of this square are at points $1, i, -1$ and $-i$ (which are the fixed points of $\mathbf{AB}, \mathbf{A}, \mathbf{BA}$ and \mathbf{B} , respectively). We have also indicated the centers of each square together with the resulting tree (this is called the dual graph of the tessellation), which turns out to be a Farey tree (Schröder 2006). Each line connecting two of these centers represents the action of a word (with alphabet $\{\mathbf{A}, \mathbf{B}\}$).

To give an explicit construction rule for the admissible words, we proceed as follows. First, we arbitrarily choose a side of the fundamental square and assign to it the value 0. Then the other three sides are numbered clockwise as 1, 2 and 3. It is easy to convince oneself that

Table 1. Explicit rules to obtain the center z_{n+1} from z_n in the tiling by hyperbolic squares. We have indicated the corresponding transformations, which depend on the color jump and the sides crossed by going from z_n to z_{n+1} .

Side	Red \rightarrow Yellow			Yellow \rightarrow Red		
	T	\mathbf{A}_{n+1}	\mathbf{B}_{n+1}	T	\mathbf{A}_{n+1}	\mathbf{B}_{n+1}
0	\mathbf{A}_n	\mathbf{B}_n	$\mathbf{A}_n \mathbf{B}_n \mathbf{A}_n^{-1}$	\mathbf{A}_n^{-1}	\mathbf{A}_n	$\mathbf{A}_n^{-1} \mathbf{B}_n \mathbf{A}_n$
1	\mathbf{B}_n	$\mathbf{B}_n \mathbf{A}_n \mathbf{B}_n^{-1}$	\mathbf{B}_n	\mathbf{B}_n^{-1}	$\mathbf{B}_n^{-1} \mathbf{A}_n \mathbf{B}_n$	\mathbf{B}_n
2	\mathbf{B}_n^{-1}	$\mathbf{B}_n^{-1} \mathbf{A}_n \mathbf{B}_n$	\mathbf{B}_n	\mathbf{B}_n	$\mathbf{B}_n \mathbf{A}_n \mathbf{B}_n^{-1}$	\mathbf{B}_n
3	\mathbf{A}_n^{-1}	\mathbf{A}_n	$\mathbf{A}_n^{-1} \mathbf{B}_n \mathbf{A}_n$	\mathbf{A}_n	\mathbf{A}_n	$\mathbf{A}_n \mathbf{B}_n \mathbf{A}_n^{-1}$

this assignment fixes once and for all the numbering for the sides of all the other squares in the tessellation. However, these squares can be distinguished by their orientation (as seen from the corresponding center): the clockwise oriented ones are filled in red, while the counterclockwise ones are filled in yellow. In short, we have determined a fundamental coloring of the tessellation (Grünbaum and Shepard 1987).

To obtain a center z_{n+1} from a previous one z_n , one looks first at the corresponding color jump. Next, the matrix that takes z_n into z_{n+1} depends on the numbering of the side (0, 1, 2, or 3) one must cross, and appears in the column labeled T in table 1. The next generation is obtained in much the same way, except for the fact that \mathbf{A}_n and \mathbf{B}_n must be replaced by \mathbf{A}_{n+1} and \mathbf{B}_{n+1} , respectively, as indicated in the table. In obtaining recursively any word, the origin is denoted as z_0 and the matrices \mathbf{A}_0 and \mathbf{B}_0 coincide with \mathbf{A} and \mathbf{B} .

One can then construct any word step by step. For example, the word that transforms z_0 into z_6 in the zig-zag path sketched in figure 2 results:

$$\begin{aligned}
 z_0 \rightarrow z_1: & \mathbf{A}, \\
 z_1 \rightarrow z_2: & \mathbf{A} \mathbf{B}^{-1} \mathbf{A}^{-1}, \\
 z_2 \rightarrow z_3: & \mathbf{A} \mathbf{B}^{-1} \mathbf{A}^{-1}, \\
 z_3 \rightarrow z_4: & \mathbf{A} \mathbf{B}^{-1} \mathbf{B}^{-1} \mathbf{A} \mathbf{B} \mathbf{B} \mathbf{A}^{-1}, \\
 z_4 \rightarrow z_5: & \mathbf{A} \mathbf{B}^{-1} \mathbf{B}^{-1} \mathbf{A} \mathbf{B} \mathbf{B} \mathbf{A}^{-1}, \\
 z_5 \rightarrow z_6: & \mathbf{A} \mathbf{B}^{-1} \mathbf{B}^{-1} \mathbf{A} \mathbf{A} \mathbf{B}^{-1} \mathbf{A}^{-1} \mathbf{A}^{-1} \mathbf{B} \mathbf{B} \mathbf{A}^{-1}.
 \end{aligned} \tag{7}$$

For this path, the final result of applying the recipes in table 1 can be condensed into the rules

$$\mathbf{A}_{n+1} = \mathbf{A}_n \mathbf{B}_n^{-1} \mathbf{A}_n^{-1}, \quad \mathbf{B}_{n+1} = \mathbf{A}_n \mathbf{B}_n^{-1} \mathbf{A}_n^{-1} \mathbf{A}_n^{-1} \mathbf{A}_n \mathbf{B}_n \mathbf{A}_n^{-1} \tag{8}$$

(and analogous ones for \mathbf{A}_n^{-1} and \mathbf{B}_n^{-1}), when the generation n is odd (i.e. the jump is red \rightarrow yellow), while

$$\mathbf{A}_{n+1} = \mathbf{A}_n, \quad \mathbf{B}_{n+1} = \mathbf{B}_n, \tag{9}$$

when the generation is even (i.e. yellow \rightarrow red). With this substitution rule, we can associate a matrix \mathbf{T} (Godrèche and Luck 1992, Peng *et al* 1993) such that each line of \mathbf{T} gives the number of letters (\mathbf{A} , \mathbf{B} , \mathbf{A}^{-1} and \mathbf{B}^{-1}) that appear in the transformations (8) and (9). This matrix then reads as

$$\mathbf{T}_{\text{odd}} = \begin{pmatrix} 1 & 0 & 1 & 1 \\ 2 & 1 & 3 & 1 \\ 1 & 1 & 1 & 0 \\ 3 & 1 & 2 & 1 \end{pmatrix}, \quad \mathbf{T}_{\text{even}} = \begin{pmatrix} 1 & 0 & 0 & 0 \\ 0 & 1 & 0 & 0 \\ 0 & 0 & 1 & 0 \\ 0 & 0 & 0 & 1 \end{pmatrix}. \tag{10}$$

Because \mathbf{T}_{even} produces a trivial effect, we concentrate on \mathbf{T}_{odd} , whose eigenvalues are $2 + \sqrt{5}$, $2 - \sqrt{5}$, 1 and -1 . Since one of the eigenvalues is greater than 1 and the others

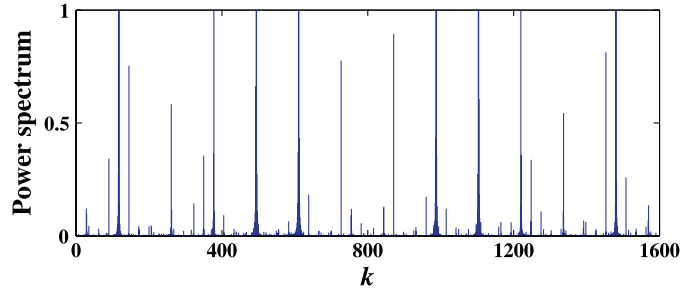


Figure 3. Normalized power spectrum for a word in the zig-zag path shown in figure 2 but with 1600 letters.

have an absolute value less than or equal to unity (with at least one of modulus 1), the substitution possesses the Salem property (Salem 1963). This is weaker than the well-known Pisot property (Pisot 1938), which is fulfilled when one of the eigenvalues of the matrix \mathbf{T} is greater than 1 and all the others are smaller than unity in modulus. Roughly speaking, only systems with the Pisot or the Salem properties present nontrivial characteristics where quasiperiodicity is concerned (Bertin *et al* 1992).

The characterization of the QP behavior of these structures is a relevant issue (Bombieri and Taylor 1987, Severin and Riklund 1989, Luck 1989, Cheng and Savit 1990). We do not enter here into a detailed analysis; our purpose is rather to give some hints that we hope will stimulate further discussion.

Given the structural model of the superlattice we deal with, we can loosely interpret each layer in the system as a kind of diffraction center. We have then four different types of centers and assign to each of them a fixed amplitude. This assignment is otherwise arbitrary and does not change any essential conclusion. In consequence, we employ the quartic roots of the identity, so that

$$\mathbf{A} \mapsto +i, \quad \mathbf{B} \mapsto +1, \quad \mathbf{A}^{-1} \mapsto -i, \quad \mathbf{B}^{-1} \mapsto -1. \quad (11)$$

In this way, given a word of N letters (represented by the transfer matrix \mathbf{M}), we turn it into a numerical sequence $w(j)$ by using (11). Next, we calculate the discrete Fourier transform of that sequence as

$$W_N(k) = \frac{1}{\sqrt{N}} \sum_{j=0}^{N-1} w(j) \exp\left(-\frac{2\pi i j k}{N}\right), \quad (12)$$

where $k = 0, 1, \dots, N - 1$. The quantity $S_N(k) = |W_N(k)|^2$ is just the power spectrum (or a structure factor) plotted in figure 3 for a word of 1600 letters that starts at the origin. The gross features of the spectrum are seen to be humps separated by almost empty regions. Inside these humps, there is a blurred structure built up of packed delta-spikes. The dominant peaks tend to be isolated and larger.

From a rigorous viewpoint, the only well-defined concept attached to the Fourier spectrum is its spectral measure. If we define

$$d\nu_N(k) = S_N(k) dk, \quad (13)$$

we will be concerned with the nature of the limit

$$d\nu(k) = \lim_{N \rightarrow \infty} d\nu_N(k), \quad (14)$$

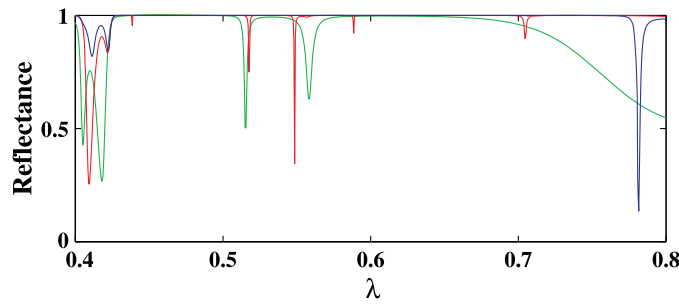


Figure 4. Spectral reflectance for the third (green), fifth (red) and seventh (blue) generations of the zig-zag path shown in figure 2. The wavelength is expressed in microns.

which corresponds to an infinite structure and a continuous variable k . Just as any positive measure, (14) has a unique decomposition (Reed and Simon 1980)

$$d\nu(k) = d\nu_{pp}(k) + d\nu_{ac}(k) + d\nu_{sc}(k) \tag{15}$$

into its pure point, absolutely continuous and singular continuous parts.

The pure point part is seen in the presence of Bragg peaks, which are apparent in figure 3. For these peaks, the Fourier amplitude $S_N(k)$ grows typically as $N^{1/2}$ and constitutes a confirmation of the Salem property exhibited by these systems.

To describe the continuous part of the measure in an analytical way seems to be a hard task. However, we can introduce the integrals (Aubry *et al* 1987, Godrèche and Luck 1990)

$$\mathcal{I}_N = \int_0^{k_{\max}} \sqrt{S_N(k)} dk, \tag{16}$$

where k_{\max} is some arbitrary spectral cutoff. The nature of the limit measure is partly coded in the behavior of these quantities for large N . In fact, for an absolutely continuous measure they tend to be constant, while they scale as $\mathcal{I}_N \sim N^{-1/2}$ for a pure point measure (Godrèche and Luck 1992). A somehow intermediate behavior can be expected for the singular continuous case. For our system, we have evaluated numerically (16), finding the law

$$\mathcal{I}_N \sim N^{-\gamma}, \quad \gamma = 0.36 \pm 0.02. \tag{17}$$

This rules out the existence of an absolutely continuous component and suggests that only a singular spectrum is present. This exponent can also be related to the theory of multifractals: if the measure $d\nu(k)$ has a generalized dimension function D_k , then γ should be linearly related to D_k (Hentschel and Procaccia 1983).

The spectral reflectance (at normal incidence) is also a good tool to characterize the optical performance. In figure 4 we have represented this magnitude for the third, fifth and seventh generations of the zig-zag path sketched in figure 2. As the spectral window of interest, we take the interval 0.4–0.8 μm . In this range the refractive index of the cryolite can be considered, to a good approximation, as constant, while for the zinc selenide we use the Sellmeier-type dispersion equation in Marple (1964). As we see, the resulting systems tend to approach a reflectance unity quite fast, which confirms the presence of a bandgap. We also observe well-defined and isolated peaks, which are reminiscent of the phenomenon of localization.

As a final and rather technical remark, we note that the quotient of the hyperbolic disc by the Fuchsian group generated by **A** and **B** is a 2-orbifold of genus 0 with three cusps. Each word represents a hyperbolic transformation of the disc, and the axis of the transformation is

projected onto a closed geodesic of such an orbifold. This provides an orbifold interpretation of our QP sequences.

In summary, we have presented a fundamental scheme to generate QP sequences based on tessellations of the unit disc, which is the natural scenario to describe the performance of these systems. Apart from the intrinsic beauty of the formalism, our preliminary analysis shows that these systems exhibit exceptional physical properties linked to their amazing geometrical properties. This should not come as a surprise, given the rich interplay between physics and geometry.

Acknowledgments

The authors wish to express their warmest gratitude to E Maciá and J M Montesinos for their help and interest in the present work. Financial support from the Spanish Research Agency (Grant FIS2005-06714) is gratefully acknowledged.

References

- Aubry S, Godrèche C and Luck J M 1987 *Europhys. Lett.* **4** 639–43
Barriuso A G, Monzón J J and Sánchez-Soto L L 2003 *Opt. Lett.* **28** 1501–3
Barriuso A G, Monzón J J, Sánchez-Soto L L and Felipe A 2005 *Opt. Express* **13** 3913–20
Beardon A F 1983 *The Geometry of Discrete Groups* (Berlin: Springer)
Bellissard J, Iochum B, Scoppola E and Testard D 1989 *Commun. Math. Phys.* **125** 527–43
Bertin M J, Decomps-Guilloux A, Grandet-Hugot M, Pathiaux-Delefosse M and Schreiber J P 1992 *Pisot and Salem Numbers* (Berlin: Birkhäuser)
Bombieri E and Taylor J E 1987 *J. Phys. Colloq.* **48** C3 19–27
Chakrabarti A, Karmakar S N and Moitra R K 1995 *Phys. Rev. Lett.* **74** 1403–6
Cheng Z and Savit R 1990 *J. Stat. Phys.* **60** 383–93
Coxeter H S M 1968 *Non-Euclidean Geometry* (Toronto: University of Toronto Press)
Coxeter H S M 1996 *Math. Intell.* **18** 42–6
Ford L R 1972 *Automorphic Functions* (New York: Chelsea Publishing Company)
Godrèche C and Luck J M 1990 *J. Phys. A: Math. Gen.* **23** 3769–97
Godrèche C and Luck J M 1992 *Phys. Rev. B* **45** 176–85
Griffiths D and Steinke C 2001 *Am. J. Phys.* **69** 137–54
Grünbaum B and Shepard G C 1987 *Tilings and Patterns* (New York: Freeman)
Hattori T, Tsurumachi N, Kawato S and Nakatsuka H 1994 *Phys. Rev. B* **50** 4220–3
Hentschel H G E and Procaccia I 1983 *Physica D* **8** 435–44
Kohmoto M, Kadanoff L P and Tang C 1983 *Phys. Rev. Lett.* **50** 1870–2
Kohmoto M, Sutherland B and Iguchi K 1987 *Phys. Rev. Lett.* **58** 2436–8
Liu N H 1997 *Phys. Rev. B* **55** 3543–7
Luck J M 1989 *Phys. Rev. B* **39** 5834–49
Lusk D, Abdulhalim I and Placido F 2001 *Opt. Commun.* **198** 273–9
Maciá E 2001 *Phys. Rev. B* **63** 205421
Maciá E 2006 *Rep. Prog. Phys.* **69** 397–441
Maciá E and Rodríguez-Oliveros R 2006 *Phys. Rev. B* **74** 144202
Magnus W 1974 *Non-Euclidean Tessellations and Their Groups* (New York: Wiley)
Marple D T F 1964 *J. Appl. Phys.* **35** 539–42
Merlin R, Bajema K, Clarke R, Juang F Y and Bhattacharya P K 1985 *Phys. Rev. Lett.* **55** 1768–70
Merlin R, Bajema K, Nagle J and Ploog K 1987 *J. Phys. Colloq.* **48** C5 503–6
Monzón J J, Yonte T, Sánchez-Soto L L and Cariñena J F 2002 *J. Opt. Soc. Am. A* **19** 985–91
Ostlund S and Pandit R 1984 *Phys. Rev. B* **29** 1394–414
Peng R W, Wang M, Hu A, Jiang S S, Jin G J and Feng D 1993 *Phys. Rev. B* **52** 13310–6
Pérez-Álvarez R, Trallero-Herrero C and García-Moliner F 2001 *Eur. J. Phys.* **22** 275–86
Pisot C 1938 *Ann. Scuola Norm. Sup. Pisa* **7** 205–48
Reed M and Simon B 1980 *Methods of Modern Mathematical Physics. I: Functional Analysis* 2nd edn (New York: Academic)

- Salem R 1963 *Algebraic Numbers and Fourier Analysis* (Boston: Heath)
- Schröder M R 2006 *Number Theory in Science and Communication* 4th edn (New York: Springer)
- Severin M and Riklund R 1989 *J. Phys.: Condens. Matter* **1** 5607–12
- Spinadel V W 1999 *Nonlinear Anal.* **36** 721–45
- Sütö A 1989 *J. Stat. Phys.* **56** 525–31
- Tamura S and Nori F 1989 *Phys. Rev. B* **40** 9790
- Vasconcelos M S and Albuquerque E L 1999 *Phys. Rev. B* **59** 11128–31
- Velasco V R and García-Moliner F 2003 *Prog. Surf. Sci.* **74** 343–55
- Yeh P 1988 *Optical Waves in Layered Media* (New York: Wiley)
- Yonte T, Monzón J J, Sánchez-Soto L L, Cariñena J F and López-Lacasta C 2002 *J. Opt. Soc. Am. A* **19** 603–9
- Zieschang H, Vogt E and Coldeway H D 1980 *Surfaces and Planar Discontinuous Groups (Lecture Notes in Mathematics)* vol 835 (Berlin: Springer)